Biophysical characterization of Vpu from HIV-1 suggests a channel-pore dualism

T. Mehnert,[1] A. Routh,[1] P. J. Judge,[1] Y. H. Lam,[1] D. Fischer,[1] A. Watts,[1] and W. B. Fischer[1,2]*

[1] Biomembrane Structure Unit, Department of Biochemistry, Oxford University, Oxford OX1 3QU, United Kingdom

[2] Bionanotechnology Interdisciplinary Research Collaboration, Clarendon Laboratory, Department of Physics, Oxford University, Oxford OX1 3PU, United Kingdom

ABSTRACT

Vpu from HIV-1 is an 81 amino acid type I integral membrane protein which consists of a cytoplasmic and a transmembrane (TM) domain. The TM domain is known to alter membrane permeability for ions and substrates when inserted into artificial membranes. Peptides corresponding to the TM domain of Vpu (Vpu_{1-32}) and mutant peptides (Vpu_{1-32}-W23L, Vpu_{1-32}-R31V, Vpu_{1-32}-S24L) have been synthesized and reconstituted into artificial lipid bilayers. All peptides show channel activity with a main conductance level of around 20 pS. Vpu_{1-32}-W23L has a considerable flickering pattern in the recordings and longer open times than Vpu_{1-32}. Whilst recordings for Vpu_{1-32}-R31V are almost indistinguishable from those of the WT peptide, recordings for Vpu_{1-32}-S24L do not exhibit any noticeable channel activity. Recordings of WT peptide and Vpu_{1-32}-W23L indicate Michaelis–Menten behavior when the salt concentration is increased. Both peptide channels follow the Eisenman series I, indicative for a weak ion channel with almost pore like characteristics.

INTRODUCTION

In the last 20 years small virus proteins have been identified which enable the flux of ions (reviewed in Refs. 1–3). The roles of these viral channel forming proteins are in some cases essential for the virus (e.g., p7 from Hepatitis C Virus (HCV)[4], M2 from Influenza A) in other cases rather supportive for the viral life cycle as in the case of Vpu from Human Immunodeficiency virus type-1 (HIV-1) and therefore being classified as accessory protein.[5] These proteins are involved in the entry/exit pathway (e.g., M2 from influenza A[6,7]), in the formation of vesicles (e.g., 2B from polio virus[8]) or the amplification of viral release (Vpu from HIV-1[9]) to mention just a few of the known roles. Their topologies range from a single transmembrane (TM) domain (e.g., M2 from influenza A,[6] Vpu from HIV-1[10]) to two (p7 from HCV,[11,12] 2B from Picornavirus[13,14]) and even three domains (3a from severe acute respiratory syndrome-associated coronavirus (SARS-CoV)[15]). The size of most of the proteins is around 100 amino acids, except for 3a with a length of 274 amino acids.[15]

All these proteins have in common that they have to oligomerise to function as a channel. In some cases experiments identify specific ion channel characteristics of the proteins preferential selectivity for one type of ion, for example the cation in most of the cases. In other cases experiments find a membrane permeabilizing effect of these proteins for ions as well as substrates and thus they are seen as viroporins[2] or ionophores,[16] lacking typical ion channel characteristics such as selectivity or gating.

In this study the focus is on Vpu from HIV-1, which is an 81 amino acid type I TM protein encoded by HIV-1 (reviewed in Refs. 3,17,18). It has a hydrophobic N-terminus which contains the TM domain and a larger cytoplasmic domain of ∼54 amino acids. Structural information is available for Vpu measured in parts (reviewed in Ref. 18): the spectroscopic methods used reveal a helical motif for the TM domain and 2–3 helices in the cytoplasmic domain. Vpu is multi-functional as it induces the degradation of CD4[19] and enhances particle release at the site of the plasma membrane by forming ion channels.[20] Ion channel function has so far only been tested *in vitro*[20–22] and in expression studies with *Xenopus* oocytes.[23] From reconstitution experiments where either peptides representing the TM part of Vpu or full length Vpu are placed into black lipid bilayers it is shown that the peptide behaves almost like the full length protein with respect to Vpu's conductance levels.[24,25] In terms of the duration of the open state, the full Vpu stays longer in the open state than the Vpu peptide.[24] These studies indicate that studies on peptides will deliver results attributable to the full length protein. In contrast to M2 for which the mechanism of function is relatively straight forward no studies have yet been done for Vpu in this respect.

Vpu comprises precious few amino acids within its TM domain which poses the question what roles these amino acids fulfill in respect of a channel's functionality meaning selectivity, ion binding site or gating. For this reason short peptides corresponding to the TM domain of Vpu and three of its mutants have been synthesized and reconstituted into lipid bilayers. On the basis of the current structural 'working' model of an ion conducting bundle of Vpu[18] the following mutations have been investigated (i) a tryptophan at the outside of the bundle has been replaced by leucine, (ii) an arginine by a valine, and (iii) a serine at the C-terminus of the peptide has been replaced by an alanine. Both the arginine and the serine are supposed to point into the lumen of the pore. The mutations have been chosen so that the characteristics of the side chain, for example aromaticity and polarity, are removed but the bulkiness of the side chains is remained.

MATERIALS AND METHODS

Peptide synthesis

Vpu$_{1-32}$ peptide and its mutants

Vpu$_{1-32}$-WT, MQPIPIVAIV[10] ALVVAIIIAI[20] VVWSIVIIEY[30] RK; Vpu$_{1-32}$-W23L, MQPIPIVAIV[10] ALVVAIIIAI[20] VV**L**SIVIIEY[30] RK; Vpu$_{1-32}$-R31V, MQPIPIVAIV[10] ALVVAIIIAI[20] VVWSIVIIEY[30] **V**K; Vpu$_{1-32}$-S24L, MQPIPIVAIV[10] ALVVAIIIAI[20] VVW**L**IVIIEY[30] RK were synthesized on a Pioneer Synthesizer from Applied Biosystems Instruments using Fmoc chemistry. The chemicals were obtained from Novabiochem and Applied Biosystems (Warrington, UK). The lyophilized cleavage mixture was purified by reverse-phase HPLC using a semiprep C18 column (Hichrom) and characterized by using a Waters-Micromass TofSpec 2E time-of-flight (TOF) mass spectrometer (Waters/Micromass MS Technologies, Manchester, UK). Details of the synthesis and analysis are given elsewhere.[25]

In brief, Fmoc-PAL-PEG-PS resin was used with a deprotecting solvent of 20% piperidine in N,N-dimethylformamide (DMF) and a fourfold excess of 9-fluorenylmethoxycarbonyl-amino acids (FMOC) with coupling reagents diisopropylethylamine (DIPEA), N-hydroxybenzotriazole (HOBT), O-benzotriazole-N,N,N′,N′-tetramethyl-uronium-hexafluorophosphate (HBTU), and for double coupling N-[(dimethylamino)-1*H*-1,2,3-trianzolo[4,5-b]pyridine-1-ylmethylene]-N-methylmethanaminium hexafluorophosphate N-oxide (HATU) or benzotriazole-1-yl-oxy-tris-pyrrolidino-phosphonium-hexafluorophosphate (PyBOP). Chemicals were obtained from Novabiochem and Applied Biosystems (Warrington, UK).

The peptide was cleaved from the resin in trifluoroacetic acids (TFA) scavenger for 5 h at room temperature. The combined filtrates were evaporated under N$_2$ gas and cold ether was added to precipitate the peptide. The precipitate was centrifuged and the solvent decanted.

The lyophilized cleavage mixture was purified by reverse-phase HPLC on a C18 column (Zorbax 300SB, 4.6 × 250 mm, 300 Å pore size, Hichrom). The gradient of a mixture of trifluor ethanol (TFE) in isopropanol and acetonitrile, and MiliQ water in 0.1% TFA was used. Elution of the peptide was followed spectroscopically at 220 and 280 nm.

The exact masses of the peptides were verified by ion MALDI spectra. The correct amino acid sequence of the first 8 amino acids of the peptide was analysis by automated peptide sequencing analysis on am Applied Biosystem 494A (Warrington UK).[26]

Reconstitution and channel recordings

POPE (1-palmitoyl-2-oleoyl-*sn*-glycero-3-phosphoethanolamine) and DOPC (1,2-dioleoyl-*sn*-glycero-3-phosphocholine) (Avanti Polar Lipids, Alabaster, US) in a mixture of 1:4 was dissolved in chloroform, dried under N$_2$ gas and resuspended in *n*-decane at 20.0 mg/mL. Approximately 1 μL of the peptide dissolved in TFE (1.0 mg/mL) was added onto a Delrin cup aperture of 150 μm and dried under N$_2$ (pretreatment). The lipid suspension was brushed over the aperture to cover it. The lipid bilayer was formed by raising and lowering the level of the buffer (300 mM KCl, 5 mM K$^+$-HEPES, pH = 7.0) in the presence of a constant negative voltage (*trans* relative to *cis*) to achieve an asymmetric orientation of the peptides within the bilayer. Experiments were performed at a temperature of T = 24 ± 1°C at which all lipid components are in the liquid crystal phase. The current response was recorded using a MultiClamp 700A system from Axon Instruments (Union City, US) with data filtered at 100 Hz using a Bessel-8-pole lowpass filter.

Data analysis

Conductance histograms of recorded traces have been obtained by superimposing individual, dwell-time-weighted Gaussian distribution functions, each representing one of the recorded events. Five conductance ranges have been defined in the obtained conductance histograms [see Fig. 1(B)]. To obtain the mean open time τ_O for each conductance state cumulative dwell-time histograms have been derived and fitted with an exponential decay function: $f(t) = A\cdot\exp(-t/\tau_O)$ applying the steepest decent gradient method.[25]

For each of the specified states i ($i = 0, 1, \ldots, 4$) their mean conductivities and their relative occurrence rates ϕ_i have been determined. As the defined states possess different conductance ranges $\Delta\kappa_i$ to obtain ϕ_i the number of events $N_{ev,i}$ per state i has been normalized to $\Delta\kappa_i$, so that ϕ_i has been calculated as follows:
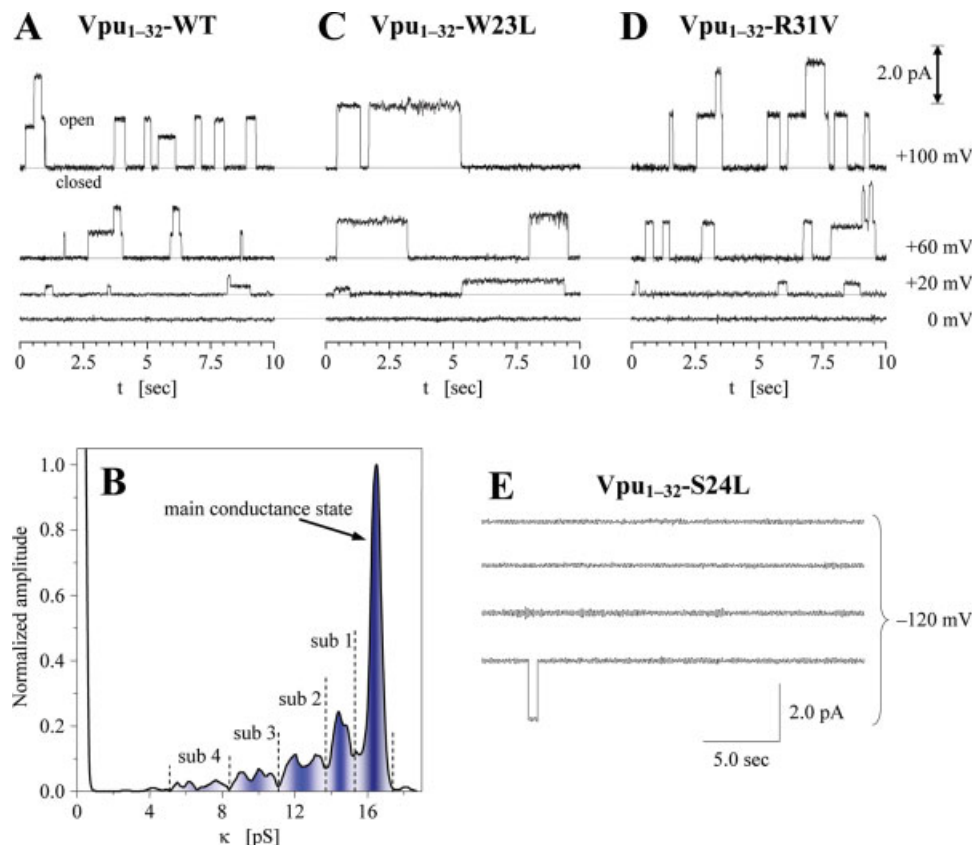
Figure 1

(A) Traces of Vpu$_{1-32}$-WT recorded using a buffer of 300 mM KCl, 5 mM K-HEPES, pH = 7.0. The data were filtered with a Bessel 8-pole lowpass filter and a cutoff of 100 Hz. (B) Conductance histogram of a trace of Vpu$_{1-32}$-WT recorded over 10 min at +100 mV comprising about 1,400 events. (C) and (D) Traces of Vpu$_{1-32}$-W23L and Vpu$_{1-32}$-R31V, respectively recorded under the same conditions as for Vpu$_{1-32}$-WT. (E) One trace of Vpu$_{1-32}$-S24L using the same buffer as stated above. [Color figure can be viewed in the online issue, which is available at www.interscience.wiley.com.]

$$\phi_i = \frac{N_{ev,i}}{\Delta\kappa_i} \cdot \left(\sum_{j=0}^{4} \frac{N_{ev,j}}{\Delta\kappa_j} \right)^{-1}, \quad (i = 0, 1, \dots, 4). \quad (1)$$

RESULTS

Channel recordings of Vpu$_{1-32}$-WT at a KCl concentration of 300 mM show frequent openings over a wide range of conductance states [Fig. 1(A)]. The calculated conductance histograms of the recorded data (900–1600 events per trace, measurement time 10–15 min) show a main-conductance state of 16.5 ± 0.09 pS [Fig. 1(B)]. The mean open time of this state is $\tau_O = 496 \pm 31.0$ ms.

Recordings of Vpu$_{1-32}$-W23L parallel the findings of Vpu$_{1-32}$-WT: (i) the frequency of events increases with increasing applied voltage, (ii) a wide range of less often appearing conductance states with lower conductivity than of the main state occurs, and (iii) observation of direct transitions between two conductance states are rare.[25] The main-conductance state is observed at $20.6 \pm$ 0.14 pS and its mean open time is $\tau_O = 795 \pm 82.4$ ms. In contrast to the other peptides, Vpu$_{1-32}$-W23L exhibits a longer opening time of the events for most of the observed conductance states. Occasionally, a flickering pattern of closings during individual open events is observed. At higher salt concentrations than 300 mM KCl the flickering intensifies significantly [Fig. 2(A)]. A conductance histogram of 25 individual events, all opening to the same conductance level of 26.8 ± 0.4 pS, recorded at $c_{KCl} = 1M$ reveals an exponential-like reduction of the occurrence rate of these closure spikes with increasing depth of them [Fig. 2(B)]. In addition, at a concentration of $2M$ KCl an increasing number of the usually barely observed direct transitions from the main-conductance state to a subconductance state with longer remaining periods in the subconductance state can be observed as shown in Figure 2(C).

Vpu$_{1-32}$-R31V repeats the pattern of WT in any respect [Fig. 1(D)]. The main-conductance state is slightly higher with 17.4 ± 0.28 pS than for Vpu$_{1-32}$-WT and its mean open time is calculated to be $\tau_O = 388 \pm 44.5$ ms.
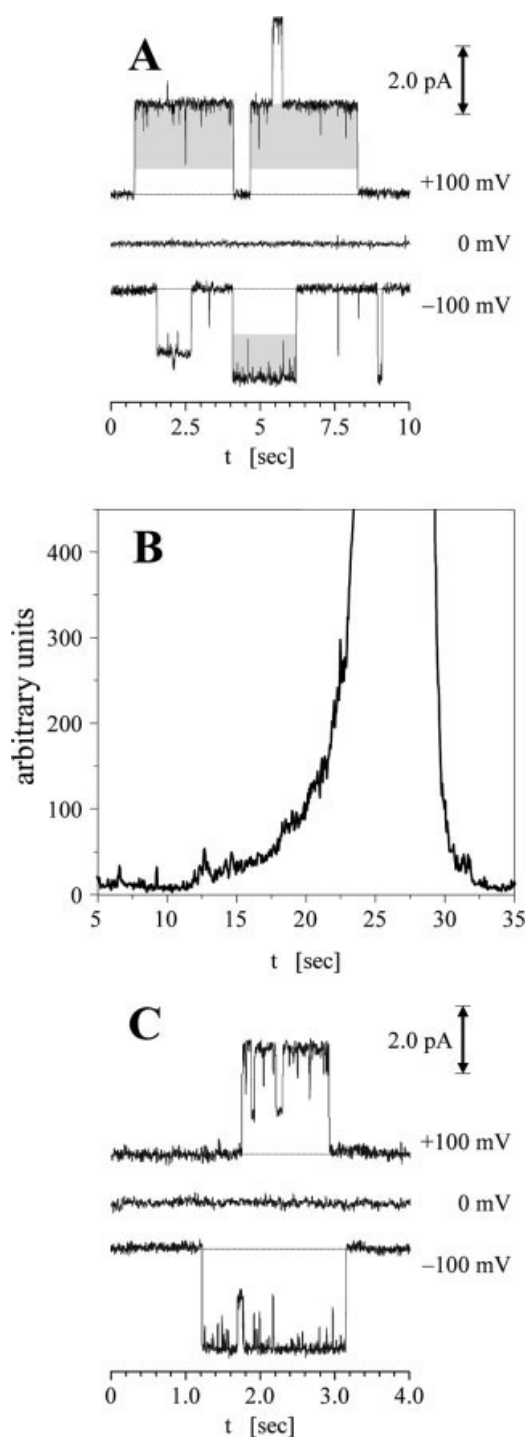
Figure 2

(**A**) Traces of bundles of Vpu$_{1-32}$-W23L using a buffer of 1M KCl, 5 mM K-Hepes, pH = 7.0. Data were filtered with a Bessel 8-pole lowpass filter and a cutoff of 100 Hz. (**B**) Superimposed histogram of 25 single main-conductance events with a sub-structure showing the channel flickering as highlighted in gray in (A). (**C**) Channel openings with several direct transitions from the main-conductance state to a sub-conductance state recorded with Vpu$_{1-32}$-W23L using a buffer of 2M KCl, 5 mM K-Hepes, pH = 7.0.

Recordings with Vpu$_{1-32}$-S24L show hardly any events suggesting that the serine residue is one of the most critical amino acids for bundles of Vpu to conduct ions. The few recorded openings have an average conductivity of 16.7 pS. By reason of the rarity of the observed events out of statistical reasons a detailed analysis has not been possible for Vpu$_{1-32}$-S24L.
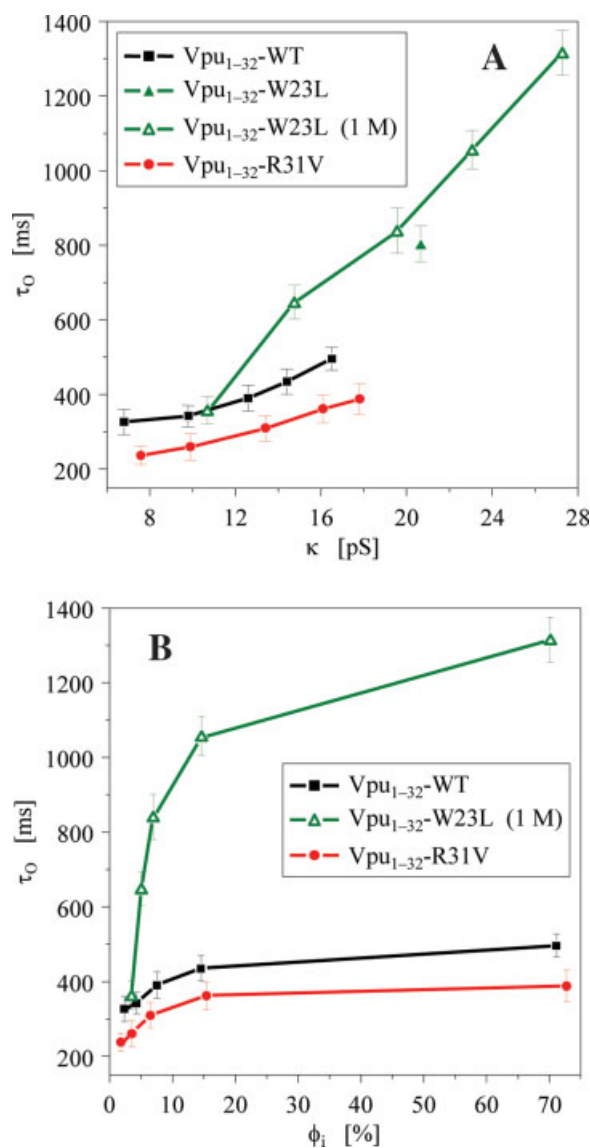
All investigated mutants (apart from the not in detail analyzed Vpu$_{1-32}$-S24L) show a similar pattern in the conductance histogram to Vpu$_{1-32}$-WT with a main state and several sub-conductance states appearing more seldom. Moreover, the occurrence rate of the sub-conductance states lessens with decreasing conductivity. Also, for all peptides a seldom appearing state above the main state is found. In contrast to Vpu$_{1-32}$-WT and Vpu$_{1-32}$-R31V, the main-conductance peak of Vpu$_{1-32}$-W23L is slightly broadened (data not shown) reflecting the flickering pattern illustrated in Figure 2(A). For all peptides investigated the current-voltage relation is ohmic (data not shown).

To be able to investigate the sub-conductance states in more detail the derived conductance histogram has been arbitrarily grouped into a main conductance range and four sub-conductance ranges [Fig. 1(B)] which will be treated as individual states. It is found that these states show a positive nearly linear correlation between the increase of the conductance and the time the state remains open [Fig. 3(A)]. For the very low sub-conductance states of Vpu$_{1-32}$-R31V and Vpu$_{1-32}$-W23L [sub-conductance state 4, see Fig. 1(B)] the mean open time is similar to Vpu$_{1-32}$-WT. All other states of Vpu$_{1-32}$-W23L appear to have notably longer opening times than Vpu$_{1-32}$-WT. Vpu$_{1-32}$-R31V shows for all states the shortest τ_O.

In addition, a comparison of the mean open time with the relative occurrence rate ϕ_i of a conductance state [Fig. 3(B)] revealed that the more often a conductance state is occupied, the longer a channel stays in the molecular conformation, representative for this state. In other words, the stability of a given conformation, related to τ_O, is proportional to the probability that a channel switches to that conformation.

Moreover, investigating the mean open time as a function of the buffer salt concentration shows that for Vpu$_{1-32}$-WT τ_O increases between 60 and 300 mM KCl and levels off to a value of 550–600 ms at higher concentrations [Fig. 4(A)]. In contrast for bundles of Vpu$_{1-32}$-W23L the increase of τ_O with increasing salt concentration between 300 mM and 2M is steeper than below 300 mM. An asymptotic approach to a maximum value is not observable within the investigated concentration range.

The relationship between salt concentration and channel activity has been recorded for Vpu$_{1-32}$-WT and Vpu$_{1-32}$-W23L in a range of $c = 0.1$–$2.0M$. The data follow Michaelis–Menten kinetics reaching saturation after around 2M. Fitting the data in a Lineweaver–Burke plot [Fig. 4(B)] determines the maximal possible conductivity for Vpu$_{1-32}$-WT to $\kappa_{max} = 29.4 \pm 0.72$ pS and the respec-
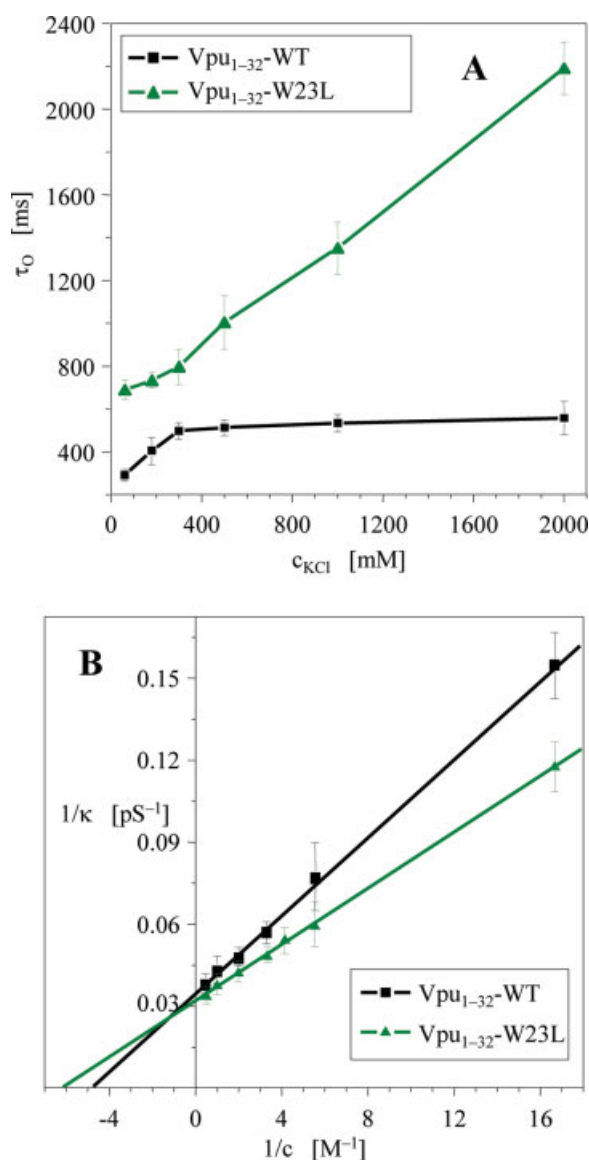
Replacing NaCl by NaBr increases slightly the conductivity of the main-conductance state (Table I). Additionally, as the sub-conductance states are also shifting it can be concluded that both cations and anions contribute to all observed conductance states. The relations between the conductivities of the sub-conductance states and of the main-conductance state $\kappa_{sub,i}/\kappa_{main}$ (i = 1, 2, 3, 4) though remain unchanged. The small shift in conductivity

Figure 3

(A) Dependency of the mean open time τ_O on the conductivity κ for the main-conductance and all sub-conductance ranges as defined in Figure 1(B). Experimental conditions: c_{KCl} = 300 mM, $c_{K-HEPES}$ = 5.0 mM, pH = 7.0. For Vpu$_{1-32}$-W23L the shown data were measured at c_{KCl} = 1M and for c_{KCl} = 300 mM only τ_O of the main conductance state is shown. (B) Correlation between the relative occurrence rates ϕ_i of a conductance state and its τ_O.

tive Michaelis–Menten constant to K_m = 209 ± 15 mM. For Vpu$_{1-32}$-W23L, κ_{max} reaches 31.8 ± 0.60 pS with a K_m of 163 ± 6 mM. The existence of a maximal conductivity implies that bundles of Vpu have channel characteristics conducting one ion at a time per binding site.

Recordings of Vpu$_{1-32}$-WT and Vpu$_{1-32}$-W23L at a constant electrolyte concentration of 500 mM with different salts [Fig. 5] show an increase in conductance in the series

$$\text{LiCl} < \text{NaCl} < \text{KCl} < \text{RbCl} < \text{CsCl}$$

Figure 4

(A) Mean open time τ_O of the main-conductance state as a function of the KCl concentration of the used buffer with 5 mM K-HEPES and pH = 7.0. (B) Lineweaver–Burke plot for Vpu$_{1-32}$-WT and Vpu$_{1-32}$-W23L to determine kinetic data for the channel activity in KCl buffer with the in (A) stated conditions. The used conductivity values refer to those of the determined main-conductance state in each trace. [Color figure can be viewed in the online issue, which is available at www.interscience.wiley.com.]
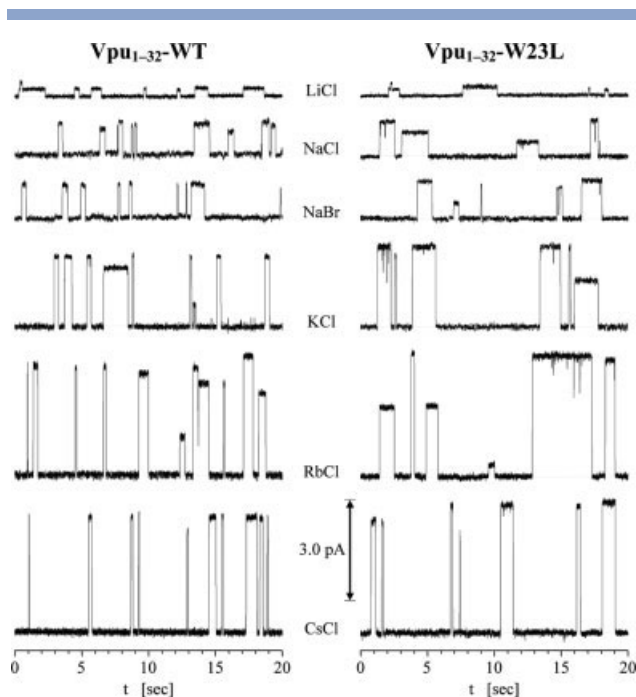
Figure 5

Traces measured with Vpu$_{1-32}$-WT and Vpu$_{1-32}$-W23L at 100 mV using different types of salt at a concentration of 500 mM. The traces were filtered with a Bessel (8-pole) lowpass filter applying a cutoff of 100 Hz.

between NaCl and NaBr ($\Delta\kappa = 0.4$ pS) and the large one between NaCl and KCl ($\Delta\kappa = 11.2$ pS) confirm that Vpu bundles are in favour (here 20 to 30 times $-11.2/0.4 = 28.5$) of conducting cations as reported earlier.[21]

DISCUSSION

With the novel method of peptide reconstitution (see Materials and Methods section) a bilayer patch with oriented peptide is achieved. The oriented alignment has been detected earlier[25] in recordings of Vpu$_{1-32}$-WT show a biphasic voltage activation of the rate of channel openings. Similar to *in vivo* conditions in the infected cell parallel aligned peptides diffuse in the membrane and assemble to form ion conducting bundles. In a follow up of this hypothesis the question arises whether the bundle, once formed, remains stable and induces ion flux by gating or the bundle dissembles and ion flux is interrupted. The latter case is a common view accepted for the conductance levels found for Vpu[27] and other membrane active peptides.[28] In this article the data support the idea of a stable bundle assembly undergoing gating characteristics.

Tryptophan mutation

Tryptophan on the outer side of TM domains of proteins is known to anchor their TM domain in the lipid membrane[29] (and references therein) because of the interaction of its indole ring with the glycerol-backbone and headgroup region of the lipid membrane.[30] This has been found in crystal structures of several membrane proteins such as bacteriorhodopsin[31,32] or the photosynthetic reaction centre[33] or gramicidin A.[34,35] Besides anchoring proteins within the membrane, for gramicidin it is also proposed that tryptophan plays a role in the conductance of ions by forming an ion binding site at the entrance of the pore.[36]

Vpu has one tryptophan at the C-terminus of its TM domain. On the basis of the current simulated models of bundles of Vpu,[22,37] the tryptophan residues would sit at a position in the membrane with the greatest packing stress (18–24 Å from the bilayer centre, as shown in electron density profiles of bilayers[38,39]). Replacing the bulky tryptophan with a small residue (leusine) may allow the bundle to expand more giving a larger pore diameter with the consequence of a larger conductance.

Vpu$_{1-32}$-W23L displays a significantly prolonged mean open time [Figs. 3 and 4(A)] which indicates a larger barrier for closure. Previous investigations have shown both that the transition rate from the closed to the open state is asymmetric in respect of 0 mV implying a dipole-orientation-dependent behavior[25] but that the closure rate is independent of the applied voltage suggesting a correlation of the closing mechanism with the lateral pressure profile of the bilayer.

To explain the long open time it needs to be considered that generally speaking in a thermodynamic equilibrium the values of all parameters with which a system can be described fluctuate around their expectation values. In this situation the further a state, characterized by its set of parameter values, is away from the equilibrium mean state the more seldom this state will be occupied by the system. This means for a system such as a bilayer plus a channel that there is an expectation value for the pressure of the bilayer in the immediate surrounding of the channel. However, the pressure will vary in time. Furthermore, the larger the difference ΔP between a certain pressure P_{close}, necessary to close a channel, and the expectation value of the bilayer pressure is the less likely this pressure will

Table I

Conductivity Measured from I/V Plots of Recordings with Vpu$_{1-32}$-WT and Vpu$_{1-32}$-W23L Using Salts with Different Monovalent Cations

Salt	WT Vpu$_{1-32}$ κ (pS)	Vpu$_{1-32}$ W23L κ (pS)
LiCl	2.4 ± 0.37	2.4 ± 0.34
NaCl	9.4 ± 0.93	10.0 ± 1.08
NaBr	9.8 ± 1.27	11.0 ± 1.16
KCl	20.6 ± 1.50	23.9 ± 1.64
RbCl	32.0 ± 2.40	36.0 ± 2.91
CsCl	34.8 ± 2.74	38.3 ± 3.42

The given uncertainty corresponds to the standard deviation obtained by a linear fit of the I/V curves comprising between 6 and 10 data points each.

occur. If one assumes that a critical force F_{close} is necessary to close a channel, according to the general equation: Force F = Pressure P × Surface S to achieve F_{close} with a large surface a small pressure is enough whereas with a small surface a large pressure is required.

Taking the tryptophan as part of the surface S against which the bilayer presses means replacing the tryptophan by leucine reduces S. Consequently, if F_{close} is almost identical for Vpu$_{1-32}$-WT and Vpu$_{1-32}$-W23L a larger pressure is required for Vpu$_{1-32}$-W23L to reach F_{close} than for Vpu$_{1-32}$-WT. Thus, for Vpu$_{1-32}$-W23L P_{close} is further away from the expectation value of the pressure of that bilayer system and consequently the closure occurs less often.

The flickering pattern observable at higher salt concentrations shows an exponential-like reduction of the occurrence rate of the closure spikes with increasing length of the spikes [Fig. 2(A)] suggesting that the maximum of the energy barrier in Vpu$_{1-32}$-W23L between closed and open state is near the conformation of the closed state rather than of the open state. The simultaneous occurrence both of the intensification of the flickering and of an increase in τ_O with increasing salt concentration leads to the conclusion that the ion pressure of the water phase exerts a non-negligible force on a Vpu channel which tries to keep the channel open. This force increases with increasing salt concentrations making it harder for a channel to overcome it and, in analogy to the earlier-given explanation of the lengthened open times of Vpu$_{1-32}$-W23L in comparison to Vpu$_{1-32}$-WT, leading to longer τ_O values at higher salt concentrations. On a molecular level, tryptophan is supposed to interact with phospholipid headgroups in the immediate environment of the channel. This interaction has an influence on the lateral mobility of the individual Vpu peptides within the bundle. Removing the tryptophan reduces this interaction leading to a higher flexibility of the Vpu peptides. Additionally, as for Vpu$_{1-32}$-WT both the flickering cannot be observed even at a concentration of $2M$ and τ_O increases only slightly at higher salt concentrations in comparison to Vpu$_{1-32}$-W23L, it can be assumed that tryptophan stabilizes the channel structure in this respect that the functionality of Vpu channels is less affected by the ion pressure of the surrounding liquid medium and thus by salt concentration variations.

Flickering in other channels[40,41] or artificial peptides[42] have been attributed to the fact that the channels are moving into sub-conductance states and get blocked by conformational changes or that analytes are passing through a channel[43,44] and thereby inhibiting temporary the flux of ions.

As a conclusion tryptophan is responsible to establish a specific energy profile for the gating mechanism of Vpu bundles. In this respect it acts as a pressure sensor which shuts the channel at the 'right' pressure without affecting the characteristic behavior of the channel (also see below). The 'right' pressure is then a function of the lipid composition which varies for example within the Golgi network.[45]

Arginine mutation

Arginine has no major impact on the gating of Vpu channels. Replacing arginine by a hydrophobic residue (Vpu$_{1-32}$-R31V) leads to very similar channel characteristics to those of Vpu$_{1-32}$-WT. The slightly higher conductance of Vpu$_{1-32}$-R31V compared to Vpu$_{1-32}$-WT may mean that the charges of the arginine in Vpu$_{1-32}$-WT which surround the mouth of the pore represent a slight conductance barrier for cations. However, it may equally be that arginine residues do not point inward the pore but maybe even outward in which case they might build hydrogen bonds with headgroups of lipids in the vicinity of a channel. In this case arginine would act as another anchor in addition to tryptophan.

Again several explanations are possible for the lower mean open time of Vpu$_{1-32}$-R31V compared to Vpu$_{1-32}$-WT: (i) Presuming that arginine points toward the channel mouth the loss of the ring of arginines removes the repelling effect of the positive charges of the arginines which reduces slightly the force necessary to close a channel and thus makes a transition from an open state to the closed state more likely. (ii) Assuming that the C-terminal part with its arginines and serines supports the formation of a water pocket which during a channel opening extends to a water column across the hydrophobic part of the channel, the removal of the hydrophilic arginines decreases the hydrophilic part of the channel and thus increase the likelihood of water chain rupture. This would lead to a reduced mean open time of a channel.

Serine mutation

The extreme rare occurrence of open events [Fig. 1(E)] or in other words the almost complete failure of Vpu$_{1-32}$-S24L bundles to conduct ions may mean that this is a further indicator, additional to the Michaelis Menten behavior [Fig. 4(B)], that Vpu possesses an ion binding site; and replacing serine by a hydrophobic residue is equal to removing Vpu's binding site. However, it may also mean that without serine the hydrophobic channel column is that long that the likelihood for filling this column with water and thus for conducting ions is extremely lessened compared to Vpu$_{1-32}$-WT. Since there are open events it is assumed that Vpu$_{1-32}$-S24L has properly inserted. Any possible structural affects based on the mutation inducing functional failure cannot be addressed further at this stage.

Channel kinetics

The finding that Vpu follows Michaelis–Menten behavior with respect to its conductivity as a function of the salt concentration suggests that ions pass one at a time and face at least one binding site during the passage. Together with the fact that Vpu follows the Eisenman sequence I[46]

indicative of a negligible electrostatic interaction with a putative binding site and rather the dehydration energy dominating, Vpu may be seen as a 'weak' ion channel. This proposal is also supported by the fact that Vpu_{1-32}-S24A hardly shows any verifiable conductance events. This also suggests that serine is the weak binding site responsible for conductivity in principle.

The Eisenman series is defined for ion conducting electrodes where the cell walls are rigid compared to the possibly more flexible walls of an ion conducting peptide assembly in the lipid membrane. The sequence of the conducting ions follows also the Hofmeister series[47] with a salting-in effect for LiCl and a salting-out effect induced by KCl. This may affect the protein/lipid system so that the density profile of the lipids is changed. While LiCl may induce a thickening of the membrane since the lipid molecules experience a salting-in effect, KCl may induce a thinning of the membrane due to the salting-out effect. The consequences would be a change in the bundle assembly from straight helices (in LiCl solution) causing low conductance to tilted helices (in KCl solution) causing higher conductance in order to avoid any mismatch of the peptide with the lipid membrane.[48,49] Thus, the ions may not only be sensed by the electrostatics within the pore but also affect the geometry of the bundle.

With the results in mind channel behavior can be described by the following two models:

A. bundles of Vpu are ion channels with Ser-24 as a weak binding site, if this binding site is removed, no verifiable conductance events can be observed.
B. bundles of Vpu are pores with a hydrophilic and hydrophobic region, whereas the hydrophilic region for WT is defined by the position of Ser. In this model the ion conductance depends on the length L of the hydrophobic region. Without Ser-24 L exceeds a critical length and therefore ions cannot be conducted. Thus, not only the diameter of the pore defined by a hydrophobic part of the pore makes the gate[50–52] but also the length of the hydrophobic stretch in the pore.

Conductance and selectivity

There are four possibilities for ion conductance when a channel is open: (i) the channel conducts only cations, (ii) the channel conducts only anions, (iii) the channel conducts cations and anions but during an individual open event it either conducts cations or anions, and (iv) within one opening event both cations and anions flow through the channel. In the case of Vpu the finding (Table I) that a shift in conductance occurs when changing the anions proves that anions contribute to the overall conductance of the channel. This rejects possibility (i). Equally changing the cations does also lead to a change in conductance, which indicates that cations contribute to the ion conductance as well, which excludes option (ii). Changing the

cation (from Na to K) leads to a stretch and shift of the overall conductance pattern rather than generating a splitting of the conductance states. This proves possibility (iii) wrong, since conductance states which can be assigned to an anion flow should remain at their original conductivity. Thus, being left with option (iv), the conclusion can be drawn that the channel conducts cations and anions during the same opening event and the conductance is in advantage of cations (one anion for 20–30 cations). In addition, it can also be concluded that the different conductance states originate from different conformational states rather than from conducting different types of ions. Since the shift is larger for changing the cations than for changing the anions the conclusion can be drawn that anions and cations contribute with different conductivities to the overall channel conductance.

It is also evident from the data that the main open state is the most long-lasting state and appears more frequently than the lower conductance states. Figure 3(B) shows an exponential-like dependency between ϕ and τ which correlates with the shape of the maximal amplitude in the histograms going from the higher to the lower conductance states.

CONCLUSIONS

From the studies it is concluded that Vpu bundles can be regarded as very weak ion channels with diffusion driven ion conductance and thus, already considerable pore characteristics. Thus according to the particle—wave dualism of light, depending on the experimental or *in vivo* conditions, for example changing lipid environment going from the ER to the Golgi or within the Golgi, Vpu bundles act either as an ion channel or a pore.

The mutant studies show that gating characteristics (flickering pattern) have no direct effect on ion channel characteristics since also the tryptophan mutation conducts ions. Thus, amino acids involved in the channel gating mechanism are independent of those defining the conductance characteristics.

ACKNOWLEDGMENTS

REFERENCES

1. Fischer WB, Sansom MSP. Viral ion channels: structure and function. Biochim Biophys Acta 2002;1561:27–45.
2. Gonzales ME, Carrasco L. Viroporins. FEBS Lett 2003;552:28–34.
3. Fischer WB. Viral membrane proteins: structure, function and drug design. In: Atassi MZ, editor. Protein reviews, Vol. 1. New York: Kluwer Academic; 2005.

4. Lohmann V, Korner F, Koch J, Herian U, Theilmann L, Bartenschlager R. Replication of subgenomic hepatitis C virus RNAs in a hepatoma cell line. Science 1999;285:110–113.

5. Emerman M, Malim MH. HIV-1 regulatory/accessory genes: keys to unraveling viral and host cell biology. Science 1998;280:1880–1884.

6. Lamb RA, Zebedee SL, Richardson CD. Influenza virus M2 protein is an integral membrane protein expressed on the infected cell surface. Cell 1985;40:627–633.

7. Sugrue RJ, Hay AJ. Structural characteristics of the M2 protein of influenza A viruses: evidence that it forms a tetrameric channel. Virology 1991;180:617–624.

8. Barco A, Carrasco L. A human virus protein, poliovirus protein 2BC, induces membrane proliferation and blocks the exocytic pathway in the yeast *Saccharomyces cerevisiae*. EMBO J 1995;14:3349–3364.

9. Klimkait T, Strebel K, Hoggan MD, Martin MA, Orenstein JM. The human immunodeficiency virus type 1-specific protein Vpu is required for efficient virus maturation and release. J Virol 1990;64:621–629.

10. Strebel K, Klimkait T, Martin MA. Novel gene of HIV-1, *vpu*, and its 16-kilodalton product. Science 1988;241:1221–1223.

11. Carrère-Kremer S, Montpellier-Pala C, Cocquerel L, Wychowski C, Penin F, Dubuisson J. Subcellular localization and topology of the p7 polypeptide of Hepatitis C virus. J Virol 2002;76:3720–3730.

12. Patargias G, Zitzmann N, Dwek R, Fischer WB. Protein-protein interactions: modeling the hepatitis C virus ion channel p7. J Med Chem 2006;49:648–655.

13. van Kuppeveld FJM, Galama JMD, Zoll J, van den Hurk PJJC, Melchers WJG. Coxsackie B3 virus protein 2B contains a cationic amphipathic helix that is required for viral RNA replication. J Virol 1996;70:3876–3886.

14. Agirre A, Barco A, Carrasco L, Nieva JL. Viroporin-mediated membrane permeabilization. Pore formation by nanostructural poliovirus 2B protein. J Biol Chem 2002;277:40434–40441.

15. Lu W, Zheng B-J, Xu K, Schwarz W, Du L, Wong CKL, Chen J, Duan S, Deubel V, Sun B. Severe acute respiratory syndrome-associated coronavirus 3a protein forms an ion channel and modulates virus release. Proc Natl Acad Sci USA 2006;103:12540–12545.

16. van Kuppeveld FJM, Melchers WJG, Kirkegaard K, Doedens JR. Structure-function analysis of coxsackie B3 virus protein 2B. Virology 1997;227:111–118.

17. Montal M. Structure-function correlates of Vpu, a membrane protein of HIV-1. FEBS Lett 2003;552:47–53.

18. Fischer WB. Vpu from HIV-1 on an atomic scale: experiments and computer simulations. FEBS Lett 2003;552:39–46.

19. Willey RL, Maldarelli F, Martin MA, Strebel K. Human immunodeficiency virus type 1 Vpu protein induces rapid degradation of CD4. J Virol 1992;66:7193–7200.

20. Schubert U, Bour S, Ferrer-Montiel AV, Montal M, Maldarelli F, Strebel K. The two biological activities of human immunodeficiency virus type 1 Vpu protein involve two separable structural domains. J Virol 1996;70:809–819.

21. Ewart GD, Sutherland T, Gage PW, Cox GB. The Vpu protein of human immunodeficiency virus type 1 forms cation-selective ion channels. J Virol 1996;70:7108–7115.

22. Cordes FS, Tustian A, Sansom MSP, Watts A, Fischer WB. Bundles consisting of extended transmembrane segments of Vpu from HIV-1: computer simulations and conductance measurements. Biochemistry 2002;41:7359–7365.

23. Coady MJ, Daniel NG, Tiganos E, Allain B, Friborg J, Lapointe J-Y, Cohen EA. Effects of Vpu expression on *Xenopus* oocyte membrane conductance. Virology 1998;244:39–49.

24. Ma C, Marassi FM, Jones DH, Straus SK, Bour S, Strebel K, Schubert U, Oblatt-Montal M, Montal M, Opella SJ. Expression, purification, and activities of full-length and truncated versions of the integral membrane protein Vpu from HIV-1. Prot Sci 2002;11:546–557.

25. Mehnert T, Lam YH, Judge PJ, Routh A, Fischer D, Watts A, Fischer WB. Towards a mechanism of function of the viral ion channel Vpu from HIV-1. J Biomol Struct Dyn 2007;24:587–596.

26. Matsudaira P. Sequence from picomole quantities of proteins electroblotted onto polyvinylidene difluoride membranes. J Biol Chem 1987;262:10035–10038.

27. Schubert U, Ferrer-Montiel AV, Oblatt-Montal M, Henklein P, Strebel K, Montal M. Identification of an ion channel activity of the Vpu transmembrane domain and its involvement in the regulation of virus release from HIV-1-infected cells. FEBS Lett 1996;398:12–18.

28. Boheim G, Hanke W, Jung G. Alamethicin pore formation: voltage-dependent flip-flop of α-helix dipoles. Biophys Struct Mech 1983;9:181–191.

29. White SH, Wimley WC. Membrane protein folding and stability: physical principles. Annu Rev Biophys Biomol Struct 1999;28:319–365.

30. de Planque MR, Kruijtzer JA, Liskamp RM, Marsh D, Greathouse DV, Koeppe RE, II, de Kruijff B, Killian JA. Different membrane anchoring positions of tryptophan and lysine in synthetic transmembrane α-helical peptides. J Biol Chem 1999;274:20839–20846.

31. Pebay-Peyroula E, Rummerl G, Rosenbusch JP, Landau EM. X-ray structure of bacteriorhodopsin at 2.5 Å from microcrystals grown in lipid cubic phases. Science 1997;277:1676–1681.

32. Luecke H, Schobert B, Richter HT, Cartailler JP, Lanyi JK. Structure of bacteriorhodopsin at 1.55 Å resolution. J Mol Biol 1999;291:899–911.

33. Deisenhofer J, Epp O, Sinning I, Michel H. Crystallographic refinement at 2.3 Å resolution and refined model of the photosynthetic reaction centre from Rhodopseudomonas viridis. J Mol Biol 1995;246:429–457.

34. Wallace BA. Structure of gramicidin A. Biophys J 1986;49:295–306.

35. Ketchem R, Roux B, Cross T. High-resolution polypeptide structure in a lamellar phase lipid environment from solid state NMR derived orientational constraints. Structure 1997;5:1655–1669.

36. Hu W, Cross TA. Tryptophan hydrogen bonding and electric dipole moments: functional roles in the gramicidin channel and implications for membrane proteins. Biochemistry 1995;34:14147–14155.

37. Moore PB, Zhong Q, Husslein T, Klein ML. Simulation of the HIV-1 Vpu transmembrane domain as a pentameric bundle. FEBS Lett 1998;431:143–148.

38. Tristram-Nagle S, Petrache HI, Nagle JF. Structure and interactions of fully hydrated dioleoylphosphatidylcholine bilayers. Biophys J 1998;75:917–925.

39. Petrache HI, Tristram-Nagle S, Gawrisch K, Harries D, Parsegian VA, Nagle JF. Structure and fluctuations of charged phosphatidylserine bilayers in the absence of salt. Biophys J 2004;86:1574–1586.

40. Colquhoun D, Sakmann B. Fluctuations in the microsecond time range of the current through single acetylcholine receptor ion channels. Nature 1981;294:464–466.

41. Seoh SA, Busath DD. Formamidinium-induced dimer stabilization and flicker block behavior in homo- and heterodimer channels formed by gramicidin A and N-acetyl gramicidin A. Biophys J 1993;65:1817–1827.

42. Thundimadathil J, Roeske RW, Guo L. Conversion of a porin-like peptide channel into a gramicidin-like channel by glycine to D-alanine substitutions. Biophys J 2006;90:947–955.

43. Movileanu L, Howorka S, Braha O, Bayley H. Detecting protein analytes that modulate transmembrane movement of a polymer chain within a single protein pore. Nat Biotechnol 2000;18:1091–1095.

44. Nestorovich EM, Danelon C, Winterhalter M, Bezrukov SM. Designed to penetrate: time-resolved interaction of single antibiotic molecules with bacterial pores. Proc Natl Acad Sci USA 2002;99:9789–9794.

45. Findlay HE, Booth PJ. The biological significance of lipid-protein interactions. J Phys: Condens Matter 2006;18:S1281–S1291.

46. Eisenman G. Cation selective glass electrodes and their mode of operation. Biophys J 1962;2(Suppl 2):259–323.

47. Baldwin RL. How Hofmeister ion interactions affect protein stability. Biophys J 1996;71:2056–2063.

48. de Planque MRR, Boots J-WP, Rijkers DTS, Liskamp RMJ, Greathouse DV, Killian JA. The effect of hydrophobic mismatch between phosphatidylcholine bilayers and transmembrane α-helical peptides depend on the nature of interfacially exposed aromatic and charged residues. Biochemistry 2002;41:8396–8404.

49. Park SH, Opella SJ. Tilt angle of a trans-membrane helix is determined by hydrophobic mismatch. J Mol Biol 2005;350:310–318.

50. Spohr E, Trokhymchuk A, Henderson D. Adsorption of water molecules in slit pores. J Electroanal Chem 1998;450:281–287.

51. Allen R, Hansen J-P, Melchionna S. Molecular dynamics investigation of water permeation through nanopores. J Chem Phys 2003;119:3905–3919.

52. Beckstein O, Sansom MSP. Liquid-vapor oscillations of water in hydrophobic nanopores. Proc Natl Acad Sci USA 2003;100:7063–7068.